Evaluation and Review of the Simultaneous Transformation Model in HSLA Steels

F. G. Caballero, C. Capdevila and C. García de Andrés

The authors are in the Department of Physical Metallurgy, Centro Nacional de Investigaciones Metalúrgicas (CENIM), CSIC, Avda. Gregorio del Amo, 8, 28040 Madrid, Spain.

This work briefly describes and evaluates one of the most complete transformation model, which deals with the non-isothermal decomposition of austenite. The model, that does not consider the effect of precipitation on phase transformations, has been experimentally validated in HSLA steels in order to evaluate how it works for microalloyed steels, where precipitation may play an important role. It has been found that the simultaneous transformation model is able to predict with an excellent agreement in microalloyed steels the formation of microstructures consisting of ferrite plus pearlite. However, the bainite formation is not successfully described in the modelling. The calculations incorrectly predict the formation of martensite instead of bainite in many situations.

1. Introduction

The production of commercial steels involves that the austenite cools continuously through the transformation temperature range. This usually leads to a final microstructure which is a mixture of many transformation products, each of which can form by a different mechanism. These reactions may overlap and interact with each other. Therefore, the modelling of the microstructure development should be capable of handling interacting reactions.

The evolution of a phase volume fraction during solid-state transformation is usually described using the classical Johnson-Mehl-Avrami theory, which has been reviewed thoroughly by Christian.[1] Jones and Bhadeshia[2] adapted this theory to deal with the formation of proeutectoid ferrite and pearlite. More recently, the model has been extended to include also non-diffussional transformations (bainite and martensite).[3] This work was part of a research project aimed the improvement of hot rolled product by physical and mathematical modelling, in which the authors were also involved. The extended model can be used to study theoretically the evolution of microstructure as a function of the alloy composition, the austenite grain size and the cooling conditions.

Modelling the phase transformations of microalloyed steels from physical principles is a very complex task. The most of the current models for the transformation behaviour of steels does not taken into account the effect of precipitates. However, those may form the basis of future models applicable to microalloyed steels. In particular, the simultaneous transformation model,[2-3] briefly described above, is at present one of the most complete continuous cooling transformation models. The aim of this work is to validate experimentally this model in HSLA steels in order to

evaluate how it works for microalloyed steels, where precipitation may play an important role.

2. Experimental Procedure

The actual chemical composition of the HSLA steels studied are given in Table 1. Alloys were supplied as hot-rolled strips. Dilatometric and metallographic analysis of the transformations that take place during continuous cooling have allowed the experimental validation of the simultaneous transformation model. An Adamel Lhomargy DT1000 high-resolution dilatometer has been used for that purpose. The dimensional variations of the specimen are transmitted via amorphous silica push-rod. These variations are measured by a linear variable differential transformer (LVDT) sensor in a gas-tight enclosure enabling testing under vacuum or in an inert atmosphere. The heating and cooling devices of this dilatometer have been also used to study previously the austenitisation condition of these steels. The DT1000 dilatometer is equipped with a radiation furnace for heating. The energy radiated by two tungsten filament lamps is focussed on the specimen by means of a bi-elliptical reflector. The temperature is measured with a 0.1 mm diameter Chromel-Alumel (Type K) thermocouple welded to the specimen. Cooling is carried out by blowing a jet helium gas directly onto the specimen surface. The helium flow-rate during cooling is controlled by a proportional servovalve. The excellent efficiency of heat transmission and the very low thermal inertia of the system ensure that the heating and cooling rates, ranging from 0.003 to 500 Ks^{-1}, remain constant.

Since austenite grain size (d_γ) exerts an important influence on the decomposition of austenite,[4] this parameter is considered a fundamental input of the model. In this sense, austenitisation conditions were fixed in each steel for the different tests performed. Cylindrical dilatometric samples of 2 mm in diameter and 12 mm in length, machined longitudinally to rolling direction, were austenitised at the temperatures listed in Table 2 for 300 seconds and subsequently were gas-quenched under helium gas flow at a cooling rate of 200 Ks^{-1}. Specimens were ground and polished by standardised techniques, and subsequently etched with picric reagent (2g picric acid + 50 ml of Teepol + a few drops of hydrochloric acid + 100 ml of water). The d_γ was estimated on micrographs by counting the number of grains intercepted by straight lines long enough to yield, in total, at least fifty intercepts. The effects of a moderately non-equiaxial structure may be eliminated by counting the intersections of lines in four or more orientations covering all the observation fields with an approximately equal weight.[5] Table 2 shows also d_γ in microns for all the steels.

Dilatometric samples of each steel were austenitised at temperatures listed in Table 2 for 300 seconds and subsequently were cooled at different cooling rates. Specimens were etched with 2% Nital solution for microstructural characterisation. Volume fraction of the different phases present in the microstructure was estimated by an unbiased systematic manual point counting procedure based upon stereological principles.[6] Quantitative measurement of ferrite grain size was determined by an intercept length procedure.[5-6]

Calculations for the decomposition of austenite in proeutectoid ferrite have been widely validated by interrupted cooling by quenching experiments. Several quench-out temperatures were selected from cooling dilatometric curves of 1 and 10 Ks^{-1} in Steel1 and Steel5 in order to investigate the progress of the $\gamma \rightarrow \alpha$ transformation.

This is determined throughout the evolution of the volume fraction of ferrite as a function of temperature. Austenite, which does not decompose before the interruption of cooling, transforms to martensite and/or bainite during quenching. Specimens from interrupted cooling experiments were polished and etched in the usual way for metallographic examination. As before, quantitative measurement of ferrite volume fraction was determined by the point counting procedure.[5-6]

3. Results and Discussion

There are two applications of the Avrami extended space idea for grain boundary nucleated reactions, the first applying to the gradual elimination of free grain boundary area and the second to the gradual elimination of volume of untransformed material.[7] Using those ideas as a starting point, Jones and Bhadeshia[2] developed a simultaneous transformation model which allows the prediction of the final microstructure and the ferrite grain size of the steel from the inputs of steel composition, prior austenite grain size and cooling schedule. The effect of eleven alloying elements is included in the model for the purposes of (a) calculating the austenite/ferrite paraequilibrium phase diagram, (b) the associated free energy changes for both paraequilibrium and diffusionless transformations and (c) the effect of substitutional solutes on the diffusivity of carbon in austenite. The austenite grains are assumed to be equiaxed and of uniform size, defined by the mean lineal intercept grain size, d_γ. Proeutectoid ferrite, pearlite and bainite are modelled with a heterogeneous simultaneous kinetics approach, whereas the martensite transformation is calculated simply as a function of the undercooling below M_s. The

necessary thermodynamic and kinetic parameters are calculated at fixed temperature steps below the paraequilibrium $Ae_3^{'}$ temperature until transformation is completed or stopped.

In that model, ferrite allotriomorphs are presumed to be discs, growing at a parabolic rate with an aspect ratio for lengthening and thickening of 3:1.[8,9] Moreover, pearlite is modelled as hemispherical particles with a linear growth rate.[10-13] For both constituents, the corresponding change in real volume after allowing for impingement with particles originating from other boundaries is:[2]

$$\Delta V_j = \left(1 - \frac{\sum_{i=1}^{n} V_i}{V}\right) \Delta V_j^e \qquad (1)$$

where V_i is the real volume of the *i*-th phase at the time *t*, *V* is the total volume and ΔV_j^e is the change in the *extended* volume of the phase *j*. The instantaneous value of ΔV_j , together with corresponding changes in the volumes of the other *n*-1 phases, can be used to calculate the total volume of each phase at the time $t+\Delta t$ in a computer implemented numerical procedure.

Avrami[14] introduced the concept of an *extended volume* to describe the volume of the particles whose growth is not impeded by impingement between particles. Particles are allowed to overlap and grow through each other. New nucleus forming in regions already transformed dubbed *phantom nuclei* are also included in the extended volume calculation. The change in extended volume of a particular phase *j* in the *i*-th time interval after the start of transformation, ΔV_j^e , is calculated from the evaluation of two factors: the change in volume due to new particles nucleated in the current

time interval, Δt; and that due to the growth of particles nucleated in all previous time intervals. The latter is quantified from the calculations of intersections of particles growing from the boundary by considering a set of planes parallel to the boundary at a distance (y) normal to the grain boundary plane. Thus, in each new time interval, the total extended volume is found by integrating, over all the planes, the transformed area on each plane due to new nuclei plus the growth of all the particles nucleated in each previous time interval,

$$\Delta V_j^e = \Delta y \sum_{y=0}^{q_j^{max}} \Delta O_{j,y} \tag{2}$$

where Δy is a small interval in y, q_j^{max} is the maximum *extended size* of a particle of phase j in a direction normal to the grain boundary plane and $\Delta O_{j,y}$ is the change in the real area intersected with the plane at y by the phase j, during the time interval t to $t+\Delta t$, and it is written as:

$$\Delta O_{j,y} = \left(1 - \frac{\sum_{i=1}^{n} O_{i,y}}{O_B} \right) \Delta O_{j,y}^e \tag{3}$$

where O_B is the total boundary area, and $\Delta O_{j,y}^e$ is the change in extended area of intersection with the same plane at y, which for allotriomorphic ferrite is given by :[2]

$$\Delta O_{j,y}^e == 2 O_b I_b \pi \eta_\alpha^2 \alpha_1^2 (\Delta t)^2 \tag{4}$$

where α_1 is the one-dimensional parabolic growth rate constant,[15] I_b is the nucleation rate per unit grain boundary area,[16] and η_α is the aspect ratio for lengthening and thickening of allotriomorphic ferrite which has a value of 3.[8,9]

The fraction of austenite boundary area transformed at each stage of the ferrite reaction is also calculated in the simultaneous transformation model. Once the boundary is saturated, the number of ferrite grains per unit volume, N_v, ceases to change. If it is assumed that each ferrite grain occupies an equal volume, the limiting value of N_v can then be used to estimate the mean ferrite grain size d_α,:

$$d_\alpha = \left(\frac{2}{3N_v}\right)^{\frac{1}{3}} \tag{5}$$

On the other hand, considering pearlite as hemispherical particles with a linear growth rate, G_P^b,[10-13] and nucleation rate per unit area, I_P,[1] the change in extended area in one time interval is given by:[2]

$$\Delta O_{j,y}^e = \pi\left(G_P^b\right)^2 O_b I_P (\Delta t)^3 \left[1 + \sum_{j=1}^{i-1} 2(i-j) - 1\right] \tag{6}$$

Parker[3] introduced calculations for the bainite volume fraction in the simultaneous transformation model. Bainite formation is modelled by adapting the Rees and Bhadeshia model[17] for boundary nucleation of sub-units at a rate per unit area of I_{α_b}.[17,18] The number of sub-units nucleated in each time interval, N_{α_b}, was given by,

$$N_{\alpha_b} = I_{\alpha_b} O_b \Delta t \tag{7}$$

In this calculation, it is assumed that each sub-unit attained its full size almost instantaneously.[19] The time required to nucleate is considered to be much greater than that for growth. The nucleation rate only concerned new sheaves starting from the boundary, while existing sheaves are automatically allowed to continue growing by addition of a new sub-unit in each time interval. The autocatalysis factor, β, introduced by Rees and Bhadeshia,[17] quantifies the successive autocatalytic nucleation of sub-units in bainite. This factor is no required in the calculation of the nucleation rate and is set to zero in the simultaneous transformation model, since only boundary nucleation of sub-units is considered. The height of the sheaves is compared with the perpendicular distances y_{iy} of a series of planes parallel to the boundary, as for other phases. The cross-sectional area of a sub-unit intersecting a plane is taken as length times width of the sub-unit (~10×0.2 μm^2). The temperature dependence of the sub-unit width is considered in calculations as determined by Chang,[20] but the influence of time is not included. Thus, the change in extended area in the *i*-th time interval is:

$$\Delta O^e_{j,y} = \sum_{j=0}^{i} N_{\alpha_b, j} \times \left(10 \times 10^{-6} \times 0.2 \times 10^{-6}\right) \times \left(\frac{T - 528}{150}\right) \tag{8}$$

where T is temperature in K.

The real volume of the bainite is then calculated as for the other phases.

Finally, the martensite transformation is modelled using the well-established theory of Koistinen and Marburger.[21] The martensite volume fraction is computed as a

function of undercooling below the martensite transformation start temperature, M_s, which is determined by solution of an equation for the driving force for the $\gamma \rightarrow \alpha'$ transformation based on quasichemical theory.[22] The model considers that once the martensite transformation is initiated, transformation to all other phases ceases.

EXPERIMENTAL VALIDATION OF THE MODEL

The simultaneous transformation model has been validated experimentally. Graphs in Fig. 1 illustrate the evolution of the predicted volume fraction of the different phases formed during continuous cooling at different rates for one of the studied steels. The experimental microstructure resulting from each cooling is shown in Fig. 2 and they are quantitatively described in the graphs of Fig. 1. Results as those illustrated in Fig. 1 allows the representation of measured and calculated volume fractions of the different phases formed during cooling at different rates in all the studied steels as shown in Fig. 3. R^2 is the square correlation factor of the experimental and calculated volume fraction of the phases. This parameter quantifies the accuracy of the model. Results for the experimental validation of ferrite and pearlite formation are represented separately of those for bainite and martensite since it has been found that the model works extremely well for ferrite and pearlite final microstructures but it is much less accurate in the prediction of those phases formed by diffusionless mechanisms.

Fig. 3.a suggests that experimental results for the volume fraction of ferrite and pearlite are in good agreement with the predicted values for all the studied steels. The accuracy of the model for the formation of both phases is of 95 %, which can be considered excellent, bearing in mind the complexity of a simultaneous

transformation model and the fact that all the steels used in the validation are microalloyed steels, when the effect of microalloyed additions is not considered in calculations.

It is known that increasing the concentration of niobium in solid solution in austenite, the formation of ferrite can be significantly retarded even though the concentration of niobium is very small.[24] On the contrary, precipitation of niobium carbides during cooling before the ferrite formation can accelerates ferrite nucleation.[23] Moreover, vanadium and titanium delay the formation of ferrite in carbon manganese steels being the effect of vanadium more severe than that of titanium.[25] The high agreement reached by the model predicting the ferrite formation in the studied steels suggests that the influence of microalloyed additions on this transformation is mainly due to the austenite grain size, which is strongly restricted by the presence of precipitates. The austenite grain is one of the input of the model.

However, Fig. 3.b indicates that bainite formation is not successfully predicted. It seems that the calculated volume fraction of bainite is insufficient and calculations incorrectly predict the formation of martensite instead of bainite in many situations. This problem is related to the fact that once the M_s temperature is reached, all the remaining austenite transforms to martensite, even before bainite transformation is completed. An example of that problem is shown in Fig.1.a. In that case (Steel1 and a cooling rate of 345 Ks^{-1}), the predicted volume fraction of bainite was less than 1 %, too small to be plotted on the graph. By contrast, experimental results show that 50 % of bainite is present in the microstructure.

Since the bainite transformation kinetics is controlled by nucleation rather than growth, it is believe that this problem must be related with an underestimation of the nucleation rate of bainite in the calculations. As it was mentioned above, the bainite

model only takes into account sheaves nucleated at the austenite grain boundary setting the autocatalysis factor to zero. However, it is known that for every successful nucleation event, a further number of nucleation sites is introduced autocatalytically.[17,18,26] Rees and Bhadeshia[17] assumed the nucleation rate due to autocatalysis to be proportional to the existing bainite volume fraction being the autocatalysis factor, the proportionality constant. Moreover, the autocatalysis factor is considered a function of the average carbon content of the steel. More recently, Singh[26] attempted to formulate the effect of autocatalysis on the total nucleation rate based on the actual mechanism of the development of the sheaf structure. This new approach suggests a total nucleation rate for bainite time-dependent. It is clear that the autocatalytic nucleation is a complex phenomena to deal with, specially under continuous cooling conditions, and an unresolved issue in the bainite transformation kinetics theory.[27]

Experimental critical temperatures for the non-isothermal decomposition of austenite into ferrite and pearlite at different cooling rates in all the steels are compared with the model predictions in Fig. 4. Ar_3 and Ar_1 critical temperatures correspond to the start and finish temperatures of the non-isothermal decomposition of austenite into ferrite and pearlite. Both temperatures are experimentally determined by dilatometry during cooling. This figure shows that the critical temperatures for the diffusional decomposition of austenite are predicted with a reasonable accuracy by the model. The influence of cooling rate as well as alloying elements on the critical temperature is reproduced successfully by the modelling. This figure demonstrates once again that the simultaneous transformation model is able to predict with an excellent agreement in microalloyed steels the formation of microstructures consisting of

ferrite plus pearlite, a microstructure of a very high proportion of the steels used in industry.

The ferrite grain size, an important factor contributing to the final mechanical properties of steels with microstructures mainly formed by ferrite and pearlite, is an output of the simultaneous transformation model. This parameter is calculated according to equation (5). The calculated and measured ferrite grain sizes of the microstructures formed at different cooling rates in all the steels are presented in Fig. 5. The model predicts reasonably the ferrite grain size of final microstructures.

The interrupted cooling results carried out to study the evolution of ferrite formation as a function of temperature in Steel1 and Steel5 are compared with the corresponding models predictions in Fig. 6. Good agreement is observed in the evolution of ferrite volume fraction in both steels at cooling rates of 1 and 10 Ks^{-1}. The transformation start temperatures and final volume fractions are reasonably predicted. Moreover, Fig. 7 shows how the non-isothermal decomposition of austenite occurs in Steel5 for a cooling rate of 1 Ks^{-1} throughout micrographs from interrupted cooling samples at different temperatures of the process. It is clear from Fig. 7.a that no transformation has taken place at 1038 K since the microstructure is formed by martensite and bainite, and no trace of ferrite has been found. Microstructure from interrupted cooling at Ar_3 temperature (Fig. 7.b) shows the first allotriomorphic ferrite grains formed during continuous cooling. That temperature was initially determined from the corresponding cooling dilatometric curve and now checked by this metallographic analysis. Figures 7.c-g show intermediate stages of the reaction. Finally, Fig. 7.h represents a microstructure formed by allotriomorphic ferrite and pearlite similar to that for the non-interrupted cooling test at 1 Ks^{-1} in Fig.

7.i. Therefore, at 899 K, the transformation has reached completion and that quench-out temperature is the Ar_1 temperature.

4. Conclusions

One of the most complete transformation model, which deals with the non-isothermal decomposition process of austenite, has been briefly described and evaluated. The model, that does not consider the effect of precipitation on phase transformations, has been experimentally validated in HSLA steels in order to evaluate how it works for microalloyed steels, where precipitation may play an important role. It has been found that the simultaneous transformation model is able to predict with an excellent agreement in microalloyed steels the formation of microstructures consisting of ferrite plus pearlite, a microstructure of a very high proportion of the steels used in industry. The transformation temperatures, the volume fraction of phases as well as the ferrite grain size are predicted with a reasonable accuracy for HSLA steels. However, the bainite formation is not successfully described in the modelling. The calculations incorrectly predict the formation of martensite instead of bainite in many situations. An underestimation of the nucleation rate of bainite in the calculus must be the reason for the lack of bainite predicted by the model. This entails a better treatments of autocatalytic nucleation, still unresolved issue in the bainite transformation kinetics theory.

5. Acknowledgements

The authors acknowledge financial support from the European Coal and Steel Community (ECSC-7210. EC/939) and the Spanish Comisión Interministerial de Ciencia y Tecnología (CICYT-MAT95-1192-CE).

6. References

1. J. W. CHRISTIAN: ‘Theory of Transformations in Metals and Alloys. Part 1’, 2nd edn, 1975, Oxford, Pergamon Press.
2. S. J. JONES and H. K .D. H. BHADESHIA: *Acta Metall.*, 1997, **45**, 2911-2920.
3. S. V. PARKER: ‘Modelling of Phase Transformation in Hot Rolled Steels’, Ph.D. Thesis, 1997, Cambridge, University of Cambridge.
4. A. K. SINHA: ‘Ferreous Physical Metallurgy’, 379; 1989, Boston, Butterworths.
5. G. F. VANDER VOORT: ‘Metallography. Principles and Practice’, 247; 1984, New York, McGraw-Hill.
6. E. E. Underwood: ‘Quantitative Stereology’, 1970, Massachusetts, Addison-Wesley Reading.
7. J. W. CAHN: *Acta Metall.*, 1956, **4**, 449-459.
8. H. K. D. H. BHADESHIA: *Progress in Materials Science*, 1985, **29**, 321-386.
9. J. R. BRADLEY and H. I. AARONSON: *Metall. Trans.* A, 1981, **12**, 1729-1741.
10. C. ZENER: *Trans. AIME*, 1946, **167**, 550.
11. M. HILLERT: *Jernkont. Ann.*, 1957, **141**, 757.
12. M. HILLERT: ‘The Mechanism of Phase Transformation in Crystalline Solids’, 231; 1969, London, Institute of Metals.
13. M. TAKAHASHI: ‘Reaustenitisation of Bainite from Steels’, Ph.D. Thesis, 1992, Cambridge, University of Cambridge.
14. M. AVRAMI: *J. Chem. Phys.*, 1939, **7**, 1103.
15. H. K. D. H. BHADESHIA, L. E. SVENSSON and B. GRETOFT: *Journal of Materials Science Letters*, 1985, **4**, 305-308.

16. R. C. REED and H. K. D. H. BHADESHIA: *Materials Science and Technology*, 1992, **8**, 421-435.
17. G. I. REES and H. K. D. H. BHADESHIA: *Materials Science and Technology*, 1992, **8**, 985-993.
18. H. K. D. H. BHADESHIA: *Journal of Physique*, 1982, **42**, (12) C4, 443-448.
19. A. ALI and H. K .D. H. BHADESHIA: *Materials Science and Technology*, 1989, **5**, 398-402.
20. L. C. CHANG and H. K .D. H. BHADESHIA: *Mater. Sci. Eng*., 1994, **A184**, L17-20.
21. D. P. KOISTINEN and R. E. MARBURGER: *Acta Metall.*, 1959, **7**, 59-60
22. H. K. D. H. BHADESHIA: *Metal Science*, 1981, **15**, 178-180.
23. M. H. THOMAS and G. M. MICHAL, in 'Solid-Solid Phase Transformations', (eds. H. I. Aaronson *et al.*), 469-473; 1981, Warrendale, MS-AIME.
24. C. FOSSAERT, G. REES, T. MAURICKX and H. K. D. H. BHADESHIA: *Metall. Trans*., 1995, **26A**, 21-30.
25. C. GARCÍA DE ANDRÉS, C. CAPDEVILA and F. G. CABALLERO: *Materials Science Forum*, 1998, **284-286**, 231-236.
26. S. B. SINGH: 'Phase Transformations from Deformed Austenite' Ph.D. Thesis, 1997, Cambridge, University of Cambridge.
27. H. K. D. H. BHADESHIA: *Materials Science and Engineering*, 1999, **A273-275**, 58-66.

Table 1 Chemical Composition, mass-%

Steels	C	Si	Mn	P	Cr	Mo	Ni	Al	Cu	Nb	Ti	V
Steel1	0.07	0.37	1.50	0.009	0.039	0.021	0.49	0.045	0.039	0.027	0.011	0.004
Steel2	0.07	0.41	1.56	0.010	0.050	0.020	0.03	-	0.019	0.053	0.003	0.084
Steel3	0.11	0.27	1.47	0.015	0.030	0.006	0.03	0.039	0.011	0.031	-	-
Steel4	0.12	0.02	1.24	0.002	0.005	0.015	0.03	0.049	0.020	0.022	0.002	0.004
Steel5	0.20	0.34	1.10	0.010	0.011	0.008	0.02	0.036	0.018	0.003	0.002	0.009

Table 2 Austenitisation Conditions

Steels	Temperature, K	d_γ, μm
Steel1	1193	9
Steel2	1211	6
Steel3	1193	4
Steel4	1178	7
Steel5	1153	10

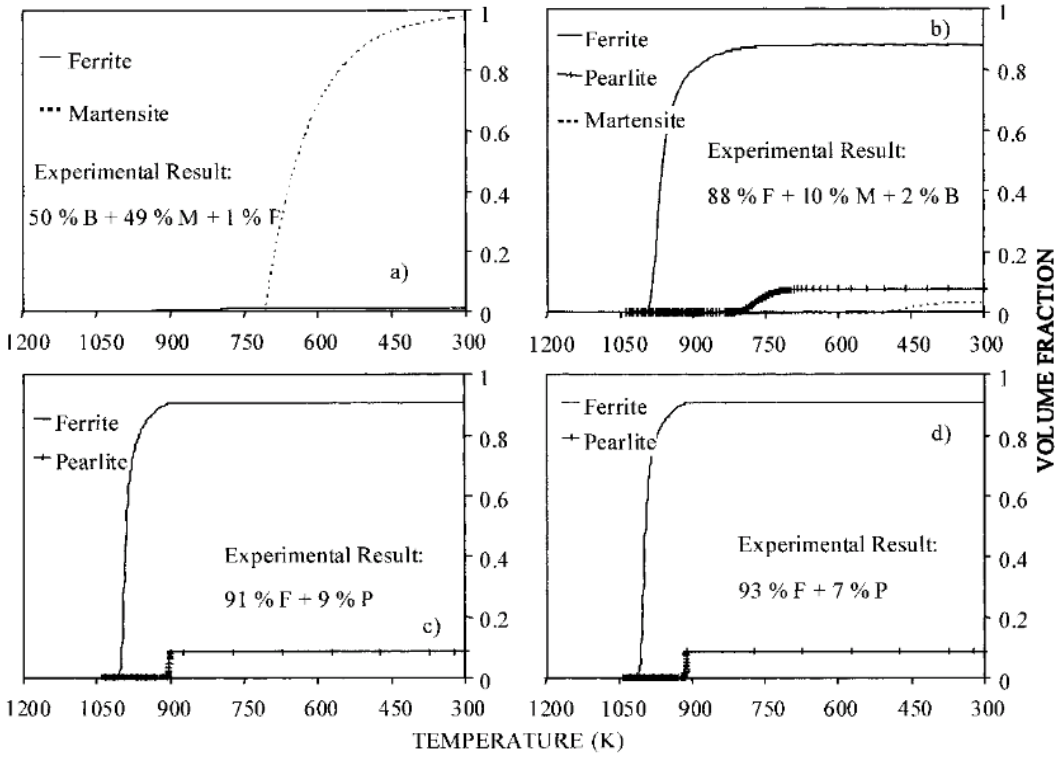

a 345 Ks^{-1}; *b* 10 Ks^{-1}; *c* 1 Ks^{-1}; *d* 0.4 Ks^{-1}.

1. **Calculated volume fraction of the different phases formed during continuous cooling in Steel1. M is martensite, B is bainite, F is ferrite and P is pearlite.**

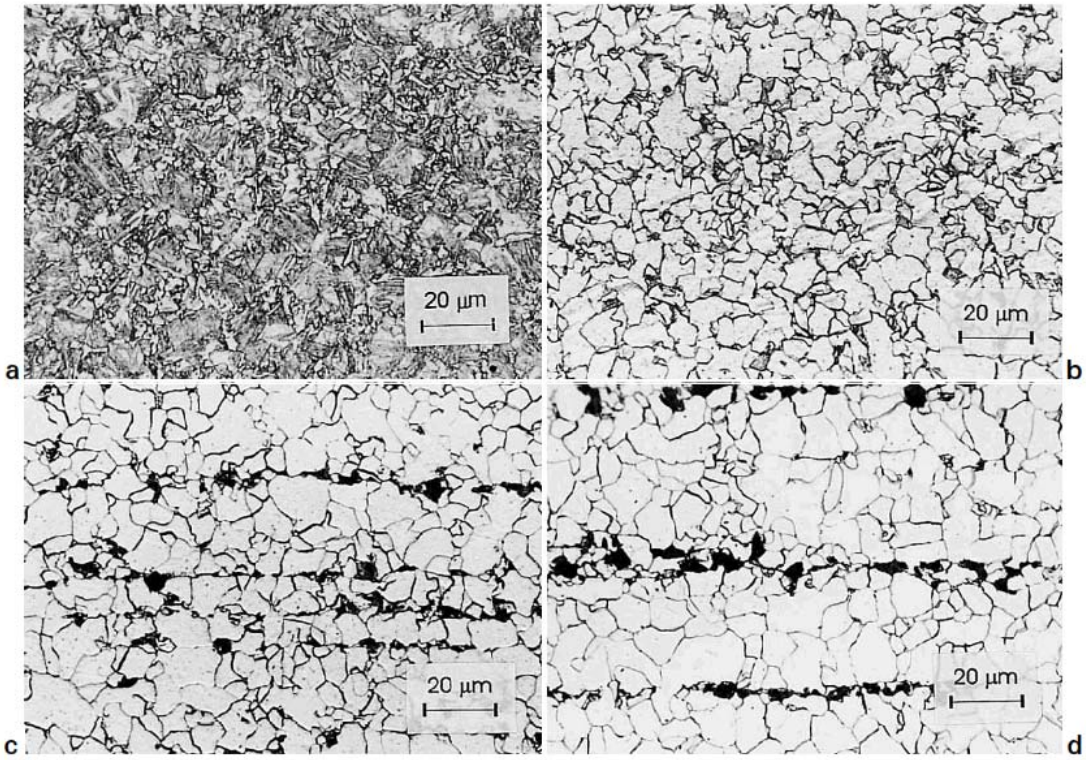

a 345 Ks^{-1}; *b* 10 Ks^{-1}; *c* 1 Ks^{-1}; *d* 0.4 Ks^{-1}.

2. **Optical micrographs of the microstructures formed during continuous cooling in Steel1.**

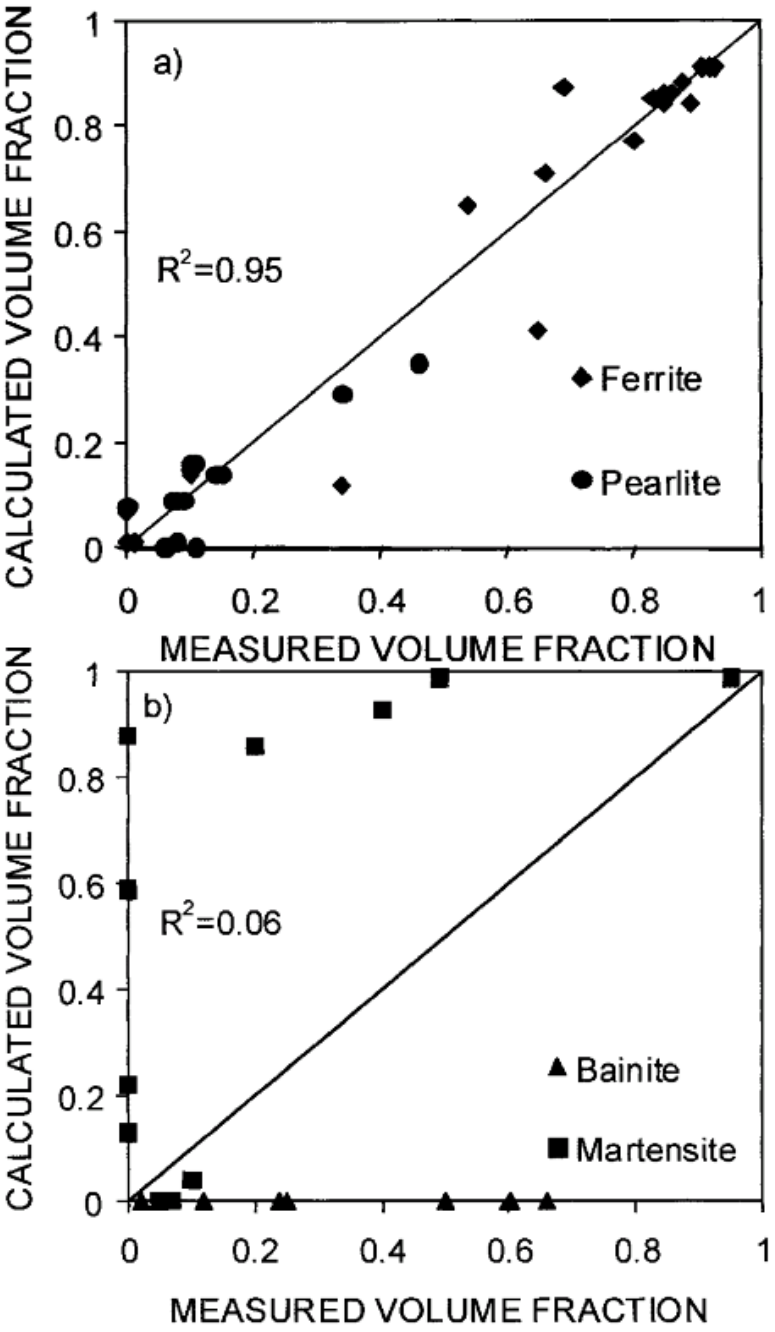

3. Comparison of measured and calculated volume fractions of the different phases formed during cooling at different rates in all the studied steels.

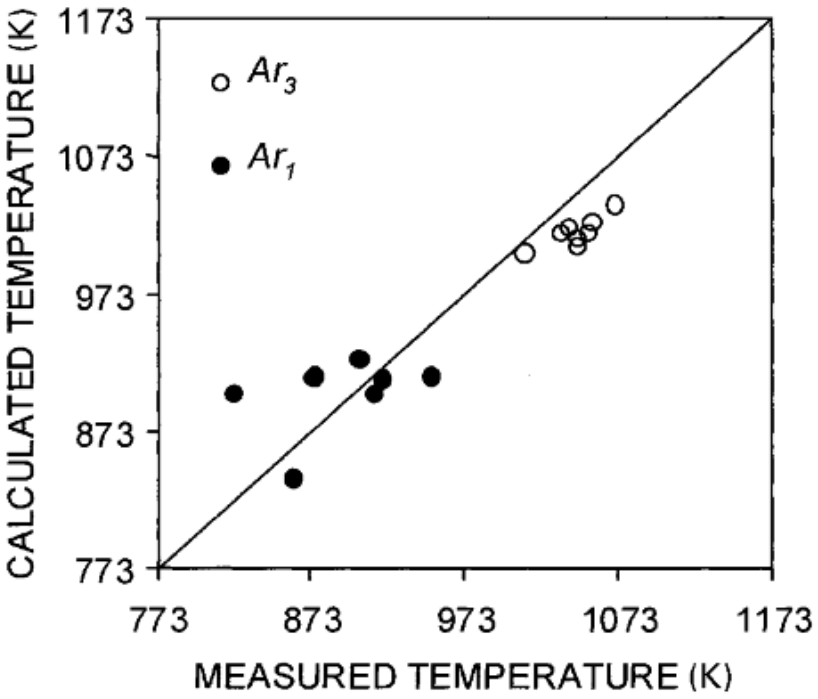

4. Comparison of calculated and experimental critical temperatures for the non-isothermal decomposition of austenite into ferrite and pearlite.

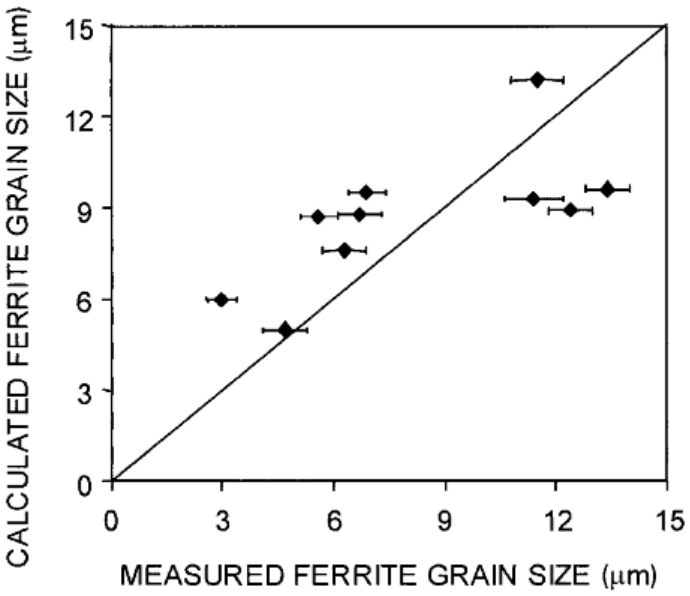

5. Comparison of measured and calculated ferrite grain sizes in microstructures formed during cooling at different rates in all the studied steels.

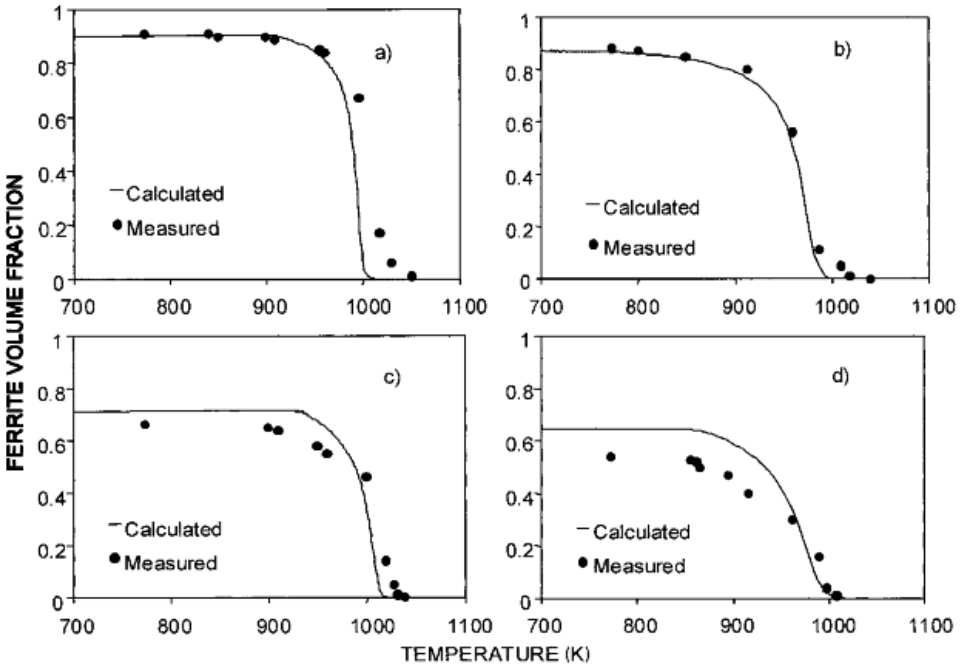

a 1 Ks^{-1}, *b* 10 Ks^{-1} in Steel1; and *c* 1 Ks^{-1}, *d* 10 Ks^{-1} in Steel5.

6. Formation of ferrite as a function of temperature during cooling at different rates in Steel1 and Steel5.

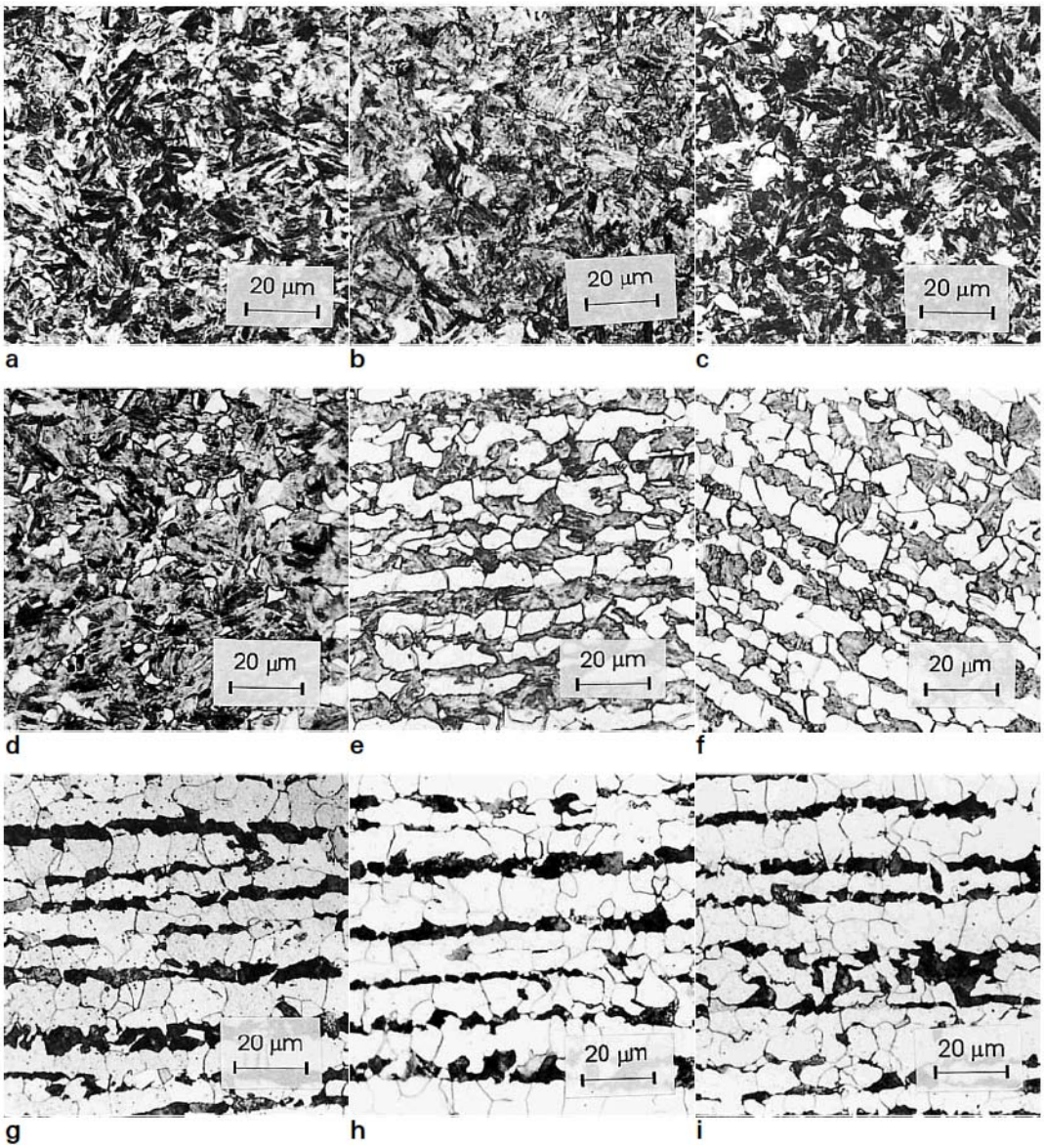

a 1038 K; *b* 1031 K (Ar_3); *c* 1027 K; *d* 1019 K; *e* 999 K; *f* 949 K; *g* 909 K; *h* 899 K (Ar_1) *i* Room temperature.

7. **Optical micrographs corresponding to the evolution of ferrite formation during cooling at a rate of 1 Ks^{-1} in Steel5.**